TRENDS IN SCIENCES 2026; 23(4): 11920
https://doi.org/10.48048/tis.2026.11920
RESEARCH ARTICLE

Transcriptomic Profiling of 6-OHDA- and Reserpine-Mediated Neurotoxicity and Neurobehavioral Change in *Caenorhabditis elegans* Model

Sukrit Promtang[1,2,*], Tanatcha Sanguanphun[3], Darunee Rodma[1,4], Rungsarit Sunan[1,4], Apinya Sayinta[1,3], Thanes Fuangfoo[2], Nattapong Snitmatjaro[2], Chaiyo Chaichantipyuth[2], Narisa Kamkaen[2], Krai Meemon[3] and Pawanrat Chalorak[5]

[1]*Anatomy Unit, Division of Basic and Medical Sciences, Faculty of Allied Health Sciences, Pathumthani University, Pathum Thani 12000, Thailand*
[2]*Faculty of Pharmacy Establishment Project, Pathumthani University, Pathum Thani 12000, Thailand*
[3]*Department of Anatomy, Faculty of Science, Mahidol University, Bangkok 10400, Thailand*
[4]*Molecular Medicine Program, Multidisciplinary Unit, Faculty of Science, Mahidol University, Bangkok 10400, Thailand*
[5]*Department of Radiological Technology and Medical Physics, Faculty of Allied Health Sciences, Chulalongkorn University, Bangkok 10330, Thailand*

([*]Corresponding author's e-mail: promtang.sukrit@gmail.com; sukrit.p@ptu.ac.th)

Received: 16 September 2025, Revised: 21 October 2025, Accepted: 28 October 2025, Published: 30 December 2025

Abstract

Neurotoxic agents such as 6-hydroxydopamine (6-OHDA) and reserpine are reported to cause neurodegenerative and neuroendocrine effects, respectively. Using the *Caenorhabditis elegans* (*C. elegans*) model, this study performs comparative transcriptomic profiling to elucidate molecular pathways that contribute to their neurotoxicity. Differentially expressed genes (DEGs) were identified following 6-OHDA and reserpine exposure, with subsequent analyses for Gene Ontology (GO) and KEGG pathway enrichment. Notably, 6-OHDA mainly disrupted ribosomal/proteasomal activity and neurodegeneration-related pathways, while reserpine primarily affected the extracellular compartment, neuropeptide-based signaling, and metabolic processes. Meta-analysis of the top 3,000 DEGs, combined with comparative enrichment network analysis of the 2 neurotoxicants using Metascape, identified critical regulatory processes, including cell development, reproduction, cytoskeletal organization, cell cycle control, metabolic pathways, and post-transcriptional regulation. In addition, protein-protein interaction (PPI) network analysis revealed eight distinct Molecular Complex Detection (MCODE) modules, which correspond to biological clusters such as regulation of translation, fatty acid metabolism, glutamate/glutamine metabolism, ceramide metabolism, sphingolipid metabolism, porphyrin metabolism, and post-transcriptional regulation. Moreover, reserpine exposure altered neurobehavioral function in the ethanol avoidance assay without inducing dopaminergic (DAergic) neurodegeneration in *C. elegans*. Overall, these findings suggest a transcriptomic framework that reports both common and unique molecular signatures of neurotoxicant-mediated neurodegeneration and behavioral alterations. These results provide valuable insights for future studies on regulatory pathways involved in PD pathogenesis.

Keywords: Transcriptome, Metascape, 6-OHDA, Reserpine, Neurotoxicity, *Caenorhabditis elegans*

Introduction

Neurodegenerative diseases are characterized by progressive dysfunction and neuronal loss in the central and peripheral nervous systems (CNS, PNS) [1]. This neuronal damage leads to various symptoms, including motor deficits, cognitive impairment, and behavioral changes [1]. Parkinson's disease (PD) is one of the

progressive neurodegenerative disorders [2]. The hallmark of PD is the selective and progressive degeneration of dopaminergic (DAergic) neurons in the substantia nigra pars compacta (SNpc), leading to a dopamine deficiency. This deficit is responsible for the motor symptoms, including bradykinesia, rigidity, and resting tremor [2]. Neurotoxicants, exogenous substances that induce damage to the CNS, are known to contribute to the PD pathogenesis [3]. Long-term usage or adverse effects of drugs often arise because they act via mechanisms shared with the disease processes, such as increasing oxidative stress or neuroinflammation [4].

6-hydroxydopamine (6-OHDA) and reserpine are neurochemical compounds commonly used to mimic the pathological features of PD in pharmacological models. 6-OHDA induces selective neurodegeneration of catecholaminergic neurons through its uptake via the dopamine transporter (DAT), resulting in rapid autooxidation and the generation of reactive oxygen species (ROS). This drives oxidative stress, mitochondrial dysfunction, and progressive neurodegeneration [5]. Furthermore, reserpine, a pharmacological agent used to treat hypertension, inhibits the vesicular monoamine transporter 2 (VMAT2), preventing monoamine neurotransmitters such as dopamine into synaptic vesicles [6]. This leads to cytosolic neurotransmitter degradation and functional depletion at the synapse, suggesting the consequences of DAergic deficiency without directly causing neuronal damage [7]. Although some studies have reported that reserpine induces oxidative stress [8], it does not replicate the key neuropathological features of PD, such as inducing mitochondrial impairment, lysosomal dysfunction, or neuroinflammation [9]. Previous study demonstrated that reserpine has toxic effects in *Caenorhabditis elegans* (*C. elegans*) by impairing neurobehavioral functions, such as reducing survival and food intake, delaying development, altering defecation cycles, and increasing locomotor rate on food [10]. Therefore, both neurotoxicants appear to be involved in neurodegenerative processes, such as PD.

Animal models can recapitulate certain aspects of PD pathology. However, they remain crucial for investigating the complex neural networks underlying brain disorders [11]. Non-mammalian species, such as nematode *C. elegans*, zebrafish, and fruit flies, have been recognized as valuable alternative models that allow results comparable to mammalian systems [12]. Among these, *C. elegans* serves as an advantageous model organism for elucidating the fundamental mechanisms underlying neurodegeneration [13]. It has been extensively employed to study aging and neurodegenerative processes, including toxin-induced DAergic neuronal degeneration relevant to PD [14,15]. Proteomic analyses have previously shown that approximately 83% of its proteome is homologous to human proteins [16]. Furthermore, its short lifespan (~20 days), optical transparency, conserved regulatory networks, and preserved neuronal pathways enhance its suitability for neurobiological research [17]. Consequently, *C. elegans* is widely used for screening and evaluating the neurotoxic effects of PD-related neurotoxicants.

Despite the increasing use of *C. elegans* as a model to study neurotoxicant-induced PD pathology, comparative transcriptomic analyses of 6-OHDA and reserpine remain limited. This study hypothesizes that both neurotoxicants can offer valuable insights into the modulation of distinct and overlapping molecular pathways in *C. elegans*. To explore this, a comparative transcriptomic approach was employed to characterize the unique and shared molecular responses induced by 6-OHDA and reserpine. The primary objectives were to identify differentially expressed genes (DEGs) and to perform Gene Ontology (GO) and Kyoto Encyclopedia of Genes and Genomes (KEGG) pathway enrichment analyses for each compound exposure. Furthermore, a comparative meta-analysis using Metascape was conducted to differentiate unique and common molecular pathways, and Molecular Complex Detection (MCODE) clustering was utilized to identify core functional protein-protein interaction (PPI) complexes.

Materials and methods

C. elegans strain, its culture, synchronization, and experimental procedures

N2-Bristol (wild-type) strain of *C. elegans* was obtained from the *Caenorhabditis* Genetics Center (CGC, Minneapolis, MN, USA), while BY250 strain was kindly provided by Prof. Randy Blakely (Florida Atlantic University, USA). Both strains were cultured on nematode growth medium (NGM) agar plates seeded with *E. coli* OP50 and maintained at 20 °C in a

temperature-controlled incubator. To obtain a synchronized population, gravid worms were subjected to bleaching solution (12% (*v/v*) sodium hypochlorite and 10% (*v/v*) 1 M sodium hydroxide) for 10 min. Released embryos were collected by centrifugation, washed 3 times with M9 buffer, and subsequently placed on NGM plates without *E. coli* OP50. Incubation overnight at 20 °C enabled hatching and development to the L1 stage. L3 larvae were generated by transferring synchronized L1 worms onto NGM plates containing *E. coli* OP50 and incubating them overnight at 20 °C. Neurotoxin 6-OHDA (Sigma, St. Louis, MO, USA) was employed for induction in L3 larvae for 1 h as described in our previous study [18]. For reserpine induction, synchronized L1 larvae were exposed to reserpine (Sigma, St. Louis, MO, USA) on NGM plates supplemented with the chemical 5-fluorodeoxyuridine (FUdR) for 72 h [19]. In our study, exposure to 190 µM reserpine was found to induce ROS production and alter neurobehavioral functions.

RNA extraction and sequencing

Transcriptomic profiling was performed on 3 experimental groups: control/DMSO, 6-OHDA/DMSO, and reserpine/DMSO. Following induction, total RNA was isolated using TRIzol reagent (Ambion, Life Technologies, NY, USA). RNA concentration and purity were assessed with a NanoDrop 2000 spectrophotometer (Thermo Scientific, Waltham, MA, USA). RNA aliquot (20 µL) was submitted to GENEWIZ (Azenta Life Sciences, MA, USA) for mRNA library preparation and sequencing. Subsequent library preparation, sequencing, and bioinformatic analyses, including identification of DEGs, GO annotation, and KEGG pathway analysis, were performed according to our previously described protocols [20].

Metascape dataset analysis

Metascape (http://metascape.org) is a web-based platform compatible with all major browsers and supports *C. elegans* datasets by converting them into Gene ID-centric relational formats [21]. In this study, top 3,000 significant DEGs were selected for comparative analysis between the 6-OHDA- and reserpine-induced groups. By default, pathway enrichment analysis in Metascape integrates multiple databases, including GO, KEGG, and Reactome [21]. Pairwise similarities between enriched terms were calculated using the Kappa statistic, followed by hierarchical clustering of the similarity matrix [22]. Threshold of 0.3 was applied to partition the tree into discrete clusters, and within each cluster, the most statistically significant term (lowest *p*-value) was chosen as the representative. These representative terms were then visualized through heatmaps.

For interactome analysis, Metascape employs physical protein-protein interactions (PPI) provided in BioGrid [23]. Candidate proteins were used to construct an interaction network, which was subsequently analyzed using the MCODE algorithm [24]. Terms with a similarity score greater than 0.3 were connected by edges, with edge thickness proportional to the similarity score. All network visualizations were generated using Cytoscape version 3.10.3 using a force-directed layout [25].

Ethanol avoidance neurobehavior

Ethanol avoidance assay is a well-established approach for evaluating dopamine circuits related to neurobehaviors [26]. NGM plate preparation followed previously described protocols in our studies [18]. Briefly, worms were incubated at 20 °C for 30 min to stimulate locomotion. After incubation, the number of worms in each quadrant was recorded, and ethanol avoidance index (EAI) was calculated using the formula: EAI = [(number of worms in quadrants A and D) - (number of worms in quadrants B and C)]/ total number of worms. Worms located within the inner circle were excluded from the analysis. Each experiment was independently conducted in triplicate.

Fluorescence imaging and analysis

BY250 strain (*dat-1p::gfp*) was employed to evaluate the integrity of DAergic neurons. Preparation of worm slides for imaging followed the procedures described in our previous studies [18]. Briefly, GFP-tagged cephalic (CEP) neurons were captured. Fluorescence microscopy was performed using a Nikon epifluorescence microscope (Eclipse Ci-L; Nikon Corp., Tokyo, Japan), and images were analyzed with ImageJ software (National Institutes of Health, Bethesda, MD, USA). Each experiment was independently repeated at

least 3 times, with 15 worms per group analyzed in each replicate.

Statistics

DEGs were identified using an adjusted *p*-value (*Padj*) threshold of ≤ 0.05. GO terms were annotated based on enriched gene sets with *Padj* ≤ 0.05. For functional enrichment analysis, pairwise similarities among enriched terms were computed using the Kappa statistic, and clusters were defined using a similarity threshold of 0.3. In network visualization, MCODE terms with similarity scores greater than 0.3 were connected by edges. Comparisons between control and reserpine-induced groups were performed using a 2-tailed paired *t*-test. Statistical significance was defined as $p \leq 0.05$. All experimental values are presented as the mean ± SEM from at least 3 independent experiments and were analyzed using GraphPad Prism version 10 (GraphPad Software Inc.).

Results

RNA-seq analysis revealed enriched pathways in *C. elegans* in response to 6-OHDA and reserpine induction

To investigate the transcriptional alterations underlying the phenotypic differences between control/DMSO vs. 6-OHDA/DMSO and control/DMSO vs. reserpine/DMSO, whole-genome transcriptome sequencing was performed. DEGs, GO, and KEGG pathway enrichment analyses were subsequently conducted (**Figures 1** and **2**).

In the comparison of control/DMSO vs. 6-OHDA/DMSO, volcano plot of DEGs identified a total of 8,518 significant genes, including 2,868 downregulated and 5,650 upregulated transcripts **(Figure 1(A))**. GO enrichment analysis revealed 218 significant terms, of which top 30 were visualized in a histogram. Enriched molecular functions primarily involved structural constituent of ribosome (GO:0003735; 1 up, 64 down), structural constituent of cuticle (GO:0042302; 36 up, 18 down), sequence-specific DNA binding RNA polymerase II transcription factor activity (GO:0000981; 95 up, 25 down), endopeptidase activity (GO:0004175; 2 up, 13 down), and RNA polymerase II core promoter proximal region sequence-specific DNA binding (GO:0000978; 88 up, 30 down). Enriched cellular components included components mainly linked to cytosolic large ribosomal subunit (GO:0022625; 1 up, 35 down), cytosolic small ribosomal subunit (GO:0022627; 0 up, 23 down), collagen trimer (GO:0005581; 38 up, 18 down), extracellular region (GO:0005576; 118 up, 24 down), and integral component of plasma membrane (GO:0005887; 103 up, 11 down). Enriched biological processes were mainly associated with cytoplasmic translation (GO:0002181; 0 up, 20 down), proteasomal ubiquitin-independent protein catabolic process (GO:0010499; 0 up, 11 down), proteasome-mediated ubiquitin-dependent protein catabolic process (GO:0043161; 6 up, 30 down), intraciliary transport (GO:0042073; 12 up, 0 down), and translation (GO:0006412; 3 up, 44 down) (**Figure 1(B)**). Top 30 GO terms ranked by *p*-value are shown in **Figure 1(C)**. Overall, GO enrichment analysis suggests a robust downregulation of ribosomal/proteasome activity and protein metabolism in response to 6-OHDA exposure (**Supplementary material 1**).

KEGG enrichment analysis on the set of DEGs revealed 76 significantly enriched pathways, with DEGs predominantly annotated in neurodegeneration-related pathways, including multiple neurodegenerative diseases (ko05022; 43 up, 86 down, 10.84%), amyotrophic lateral sclerosis-ALS (ko05014; 25 up, 88 down, 9.50%), Alzheimer's disease-AD (ko05010; 36 up, 73 down, 9.16%), Parkinson's disease-PD (ko05012; 25 up, 76 down, 8.49%), Huntington disease-HD (ko05016; 26 up, 71 down, 8.15%), Prion disease (ko05020; 29 up, 66 down, 7.98%), and pathways in cancer (ko05200; 40 up, 41 down, 6.81%) (**Figure 1(D)**; **Supplementary material 2**).

In the control/DMSO vs. reserpine/DMSO comparison, volcano plot revealed 5,133 significant DEGs, comprising 3,381 downregulated and 1,752 upregulated genes (**Figure 2(A)**). GO enrichment analysis identified 120 significant terms, with top 30 represented in a histogram. Enriched molecular functions were predominantly structural constituents of cuticle (GO:0042302; 28 up, 20 down), nutrient reservoir activity (GO:0045735; 6 up, 0 down), lipid transporter activity (GO:0005319; 7 up, 0 down), mRNA 3'-UTR binding (GO:0003730; 17 up, 0 down), and serine-type endopeptidase inhibitor activity (GO:0004867; 1 up, 8 down). Enriched cellular components mainly included the extracellular region

(GO:0005576; 31 up, 81 down), collagen trimer (GO:0005581; 26 up, 18 down), pseudopodium (GO:0031143; 28 up, 2 down), cilium (GO:0005929; 5 up, 24 down), and messenger ribonucleoprotein complex (GO:1990124; 8 up, 0 down). Enriched biological processes were primarily associated with the neuropeptide signaling pathway (GO:0007218; 0 up, 19 down), collagen and cuticle development (GO:0042335; 14 up, 9 down), non-motile cilium assembly (GO:1905515; 1 up, 11 down), anatomical structure development (GO:0048856; 22 up, 16 down), and negative regulation of peptidase activity (GO:0010466; 1 up, 8 down) (**Figure 2(B)**). Top 30 GO terms ranked by *p*-value are presented in **Figure 2(C)**. Overall, GO enrichment analysis indicates a marked downregulation of the extracellular region and the neuropeptide signaling pathway, alongside an upregulation of structural cuticle constituents, including cuticle-like collagen trimers, in response to reserpine exposure (**Supplementary material 3**).

In KEGG enrichment analysis, 44 significant enriched pathways were identified, with DEGs predominantly annotated in metabolic pathways (ko01100; 93 up, 47 down, 35.90%), cell cycle (ko04110; 24 up, 11 down, 8.97%), pathways in cancer (ko05200; 18 up, 16 down, 8.72%), salmonella infection (ko05132; 13 up, 17 down, 7.69%), oocyte meiosis (ko04114; 20 up, 7 down, 6.92%), protein processing in endoplasmic reticulum (ko04141; 15 up, 10 down, 6.41%), and lysosome (ko04142; 16 up, 7 down, 5.90%) (**Figure 2(D)**); **Supplementary material 4**).

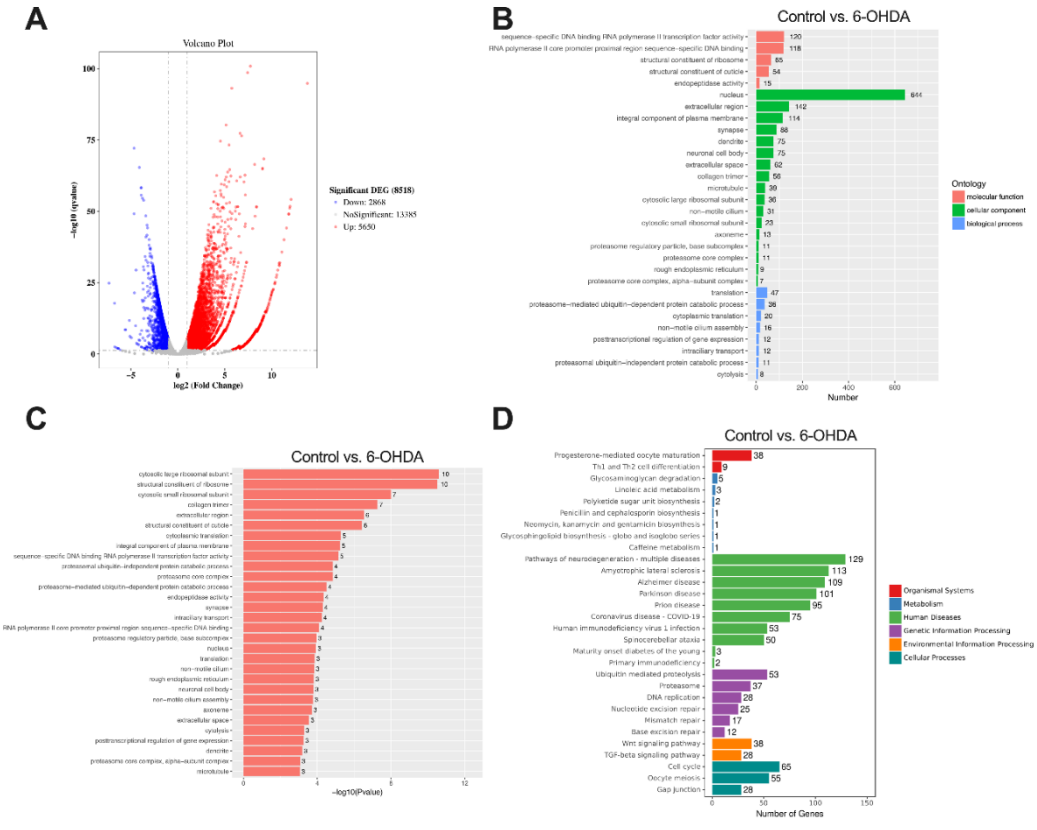

Figure 1 Transcriptomic profiling of *C. elegans* following 50 mM 6-OHDA induction compared with control. (A) Volcano plot illustrating DEGs, with upregulated genes (red dots) and downregulated genes (blue dots), identified using the DESeq2 Bioconductor package (V1.6.3) with *Padj* ≤ 0.05. (B) GO enrichment analysis showing top 30 terms based on the number of associated genes across molecular functions (e.g., sequence-specific DNA binding RNA polymerase II transcription factor activity), cellular components (e.g., nucleus), and biological processes (e.g., translation). (C) Top 30 GO terms ranked according to *p*-value, highlighting ribosomal/proteasome activity and protein metabolism. (D) Bar chart representing top 30 significantly enriched KEGG pathways, predominantly associated with neurodegeneration-related processes.

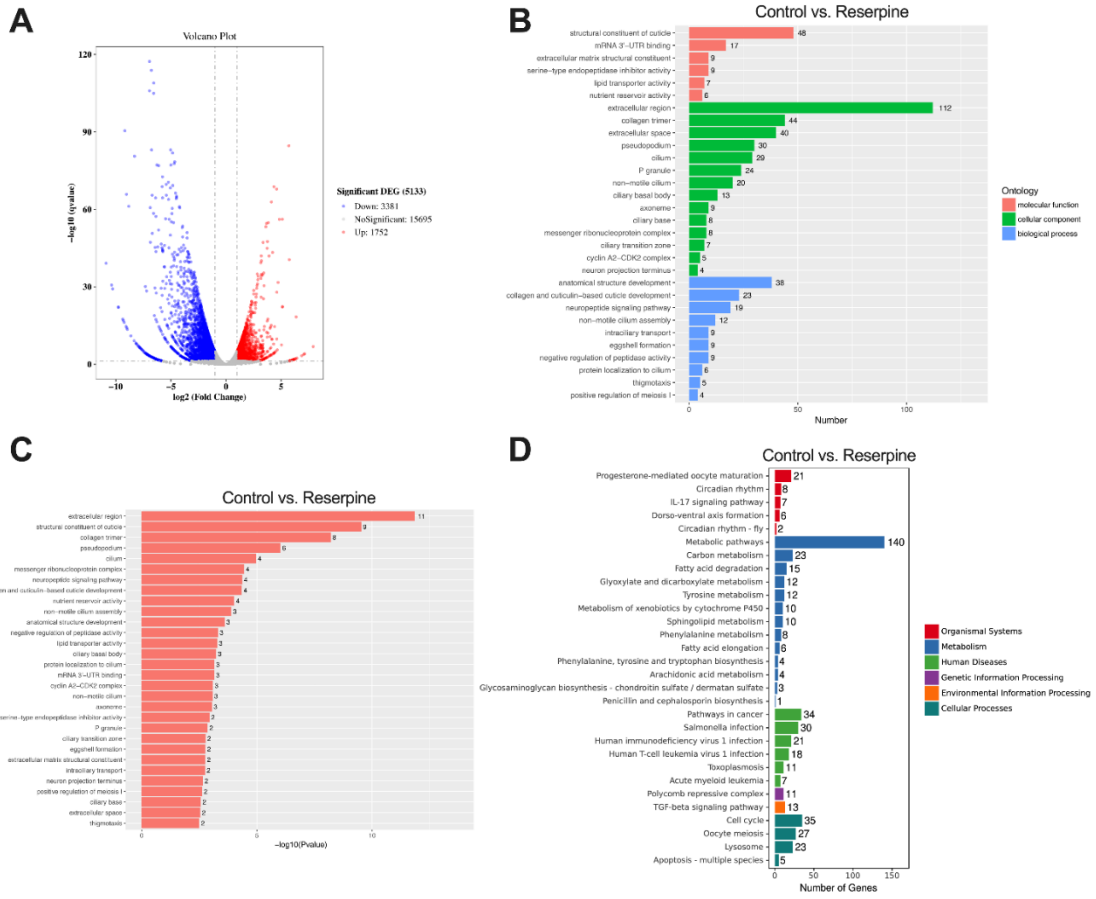

Figure 2 Transcriptomic profiling of *C. elegans* exposed to 190 µM reserpine compared with control. (A) Volcano plot illustrating DEGs, with upregulated genes shown in red and downregulated genes in blue, identified using the DESeq2 Bioconductor package (V1.6.3) with *Padj* ≤ 0.05. (B) GO enrichment analysis presenting top 30 terms based on the number of associated genes across molecular functions (e.g., structural constituents of the cuticle), cellular components (e.g., extracellular region), and biological processes (e.g., anatomical structure development). (C) Top 30 GO terms ranked according to *p*-value, involving the alteration of extracellular regions, neuropeptide signaling pathways, and structural cuticle constituents. (D) Bar chart displaying top 30 significantly enriched KEGG pathways, primarily associated with metabolic processes.

Metascape analysis revealed differential GO term enrichment between 6-OHDA- and reserpine-induced responses in *C. elegans*

Top 3,000 significant DEGs were selected for comparative analysis between the 6-OHDA- and reserpine-induced groups, of which 1,085 genes were found to overlap (**Figure 3(A)**). Submission of these gene lists to Metascape (https://metascape.org/) generated a Circos plot illustrating overlap of genes and enriched GO terms (**Figure 3(B)**). In this plot, outer arcs represented the identities of the 6-OHDA (red) and reserpine (blue) gene lists. In contrast, inner arcs reported individual genes. Shared genes were highlighted in dark orange, whereas unique genes were shown in light orange. Purple lines connected shared genes across lists, and blue lines indicated GO functional overlap, restricted to statistically significant terms with a gene set size ≤ 100.

To further examine functional enrichment, terms were visualized as a heatmap of both neurotoxicants based on –log10 (*p*-value) (**Figures 3(C)** and **3(D)**). Dark brown gradients indicated strong significance, while non-significant terms were shown in gray. Heatmap of selected GO terms revealed major clusters associated with cell development (GO:0048468), multicellular organismal reproductive process (GO:0048609), cytoskeleton organization (GO:0007010), and cell cycle regulation (GO:0051726, GO:0007049) (**Figure 3(C)**); **Supplementary material 5**). Similarly, GO parent-level analysis highlighted

enrichment in developmental processes (GO:0032502), reproductive processes (GO:0022414), cellular processes (GO:0009987), and regulation of biological processes (GO:0050789) (**Figure 3(D)**; **Supplementary material 5**). Overall, these findings indicate that both neurotoxicants predominantly affect key biological processes related to development, reproduction, cytoskeletal organization, and cell cycle regulation, resulting in their broad impact on fundamental cellular and organismal functions. Notably, the impact of 6-OHDA appears to be more pronounced than that of reserpine.

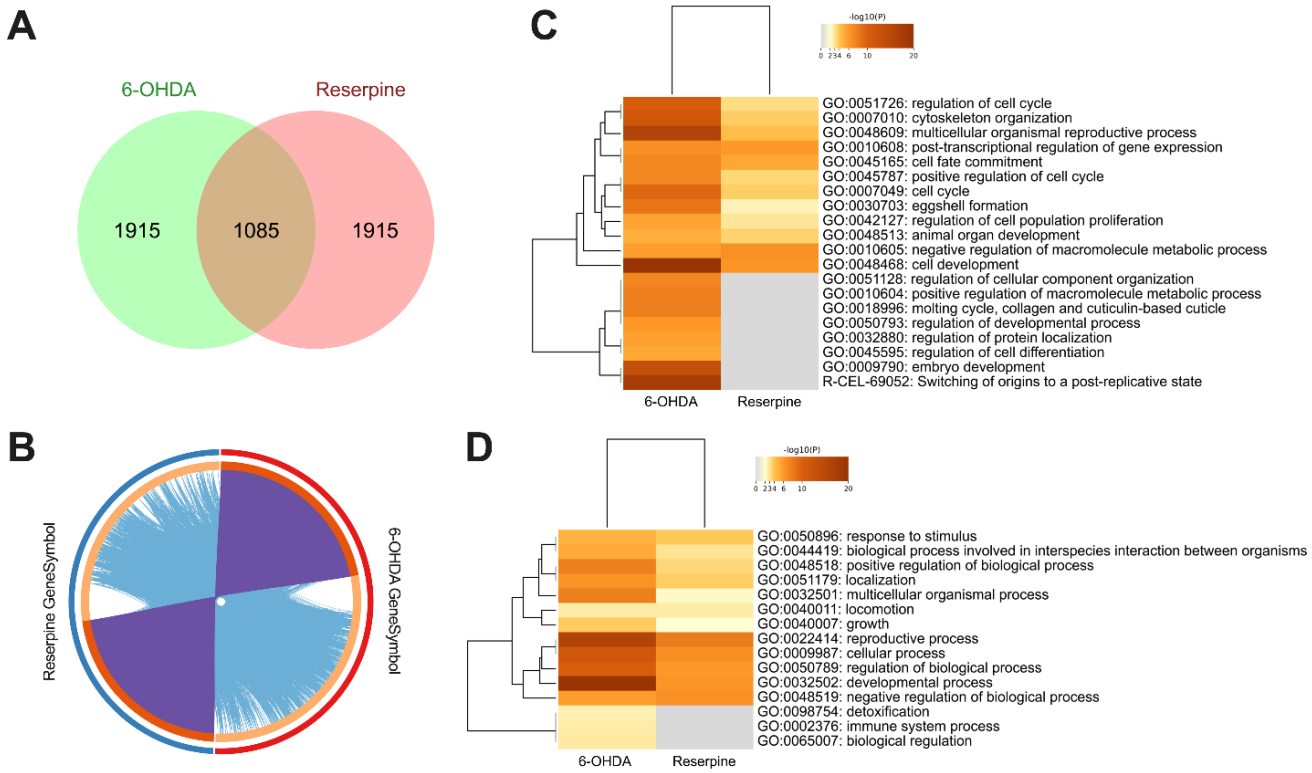

Figure 3 Top 3,000 genes significantly associated with 6-OHDA and reserpine exposure in *C. elegans* were analyzed. (A) Venn diagram displayed overlap of genes, generated using https://molbiotools.com/listcompare.php. (B) Circos plot depicted gene overlap and enriched GO terms, with 6-OHDA represented by the outer red line and reserpine by the outer blue line. (C), (D) Heatmaps displayed GO enrichment clusters of both shared and unique genes in response to 6-OHDA and reserpine exposure, emphasizing key biological processes involved in cell development, reproduction, cytoskeletal organization, and regulation of the cell cycle. Dark brown gradient indicated strong significance, whereas gray represented non-significant results.

Metascape-based enrichment clustering and protein-protein interaction network analysis of 6-OHDA- and reserpine-induced responses in *C. elegans*

Pathway clustering analysis of DEGs was performed using Metascape (https://metascape.org/) and visualized in Cytoscape v3.10.3 (https://cytoscape.org/). In the enrichment network, each node corresponded to an enriched term, where node size reflected the number of associated input genes and node color indicated cluster identity (**Figure 4(A)**; **Table 1**). Enrichment network comparison was further constructed to illustrate the functional overlap between the 6-OHDA- and reserpine-induced groups (**Figure 4(B)**).

To identify functional protein complexes, the MCODE algorithm was applied to the PPI network, resulting in the identification of 8 distinct MCODE modules representing biologically meaningful clusters (**Figure 5**; **Table 2**). Overall, these results provide a comprehensive framework for understanding the

molecular basis of both neurotoxicant-induced neurotoxicity in *C. elegans*, supporting their use in studying mechanisms and pathways involved in neurodegenerative disease pathogenesis.

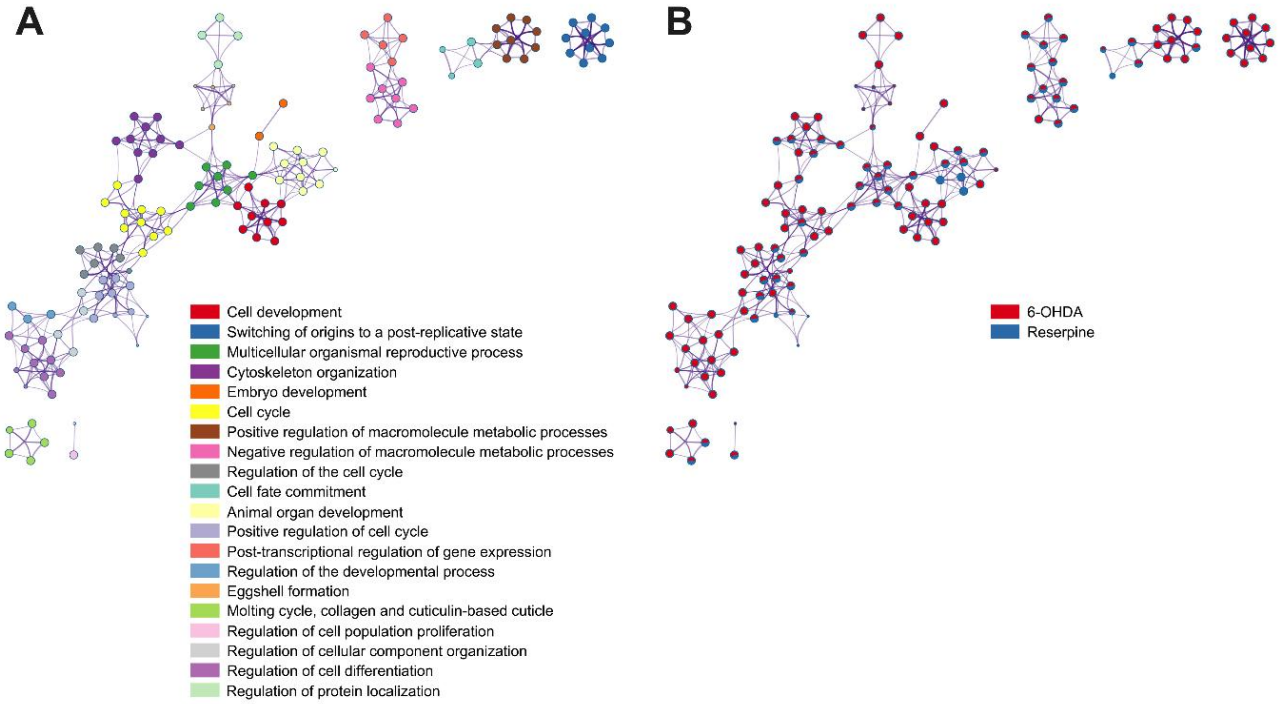

Figure 4 Enrichment network was generated using Metascape (https://metascape.org) and visualized in Cytoscape (https://cytoscape.org). (A) Network visualization illustrated the intra- and inter-cluster associations among enriched terms, with cluster annotations represented by distinct colors. (B) Enrichment network derived from the 2 gene lists, 6-OHDA and reserpine, was presented, with color coding used to indicate the respective gene list identities.

Table 1 GO enrichment across 6-OHDA and reserpine-induced groups analyzed by Metascape.

GO	Description	% in GO	Log10 (*p*-value)	Log10 (*q*-value)
GO:0048468	Cell development	9.19	−28.50	−24.64
R-CEL-69052	Switching of origins to a post-replicative state	2.32	−17.86	−14.48
GO:0048609	Multicellular organismal reproductive process	6.60	−16.51	−13.22
GO:0007010	Cytoskeleton organization	6.91	−16.48	−13.22
GO:0009790	Embryo development	7.31	−14.93	−11.92
GO:0007049	Cell cycle	7.26	−12.87	−10.40
GO:0010604	Positive regulation of macromolecule metabolic process	7.92	−12.87	−10.40
GO:0010605	Negative regulation of macromolecule metabolic process	8.13	−12.51	−10.10
GO:0051726	Regulation of the cell cycle	4.37	−12.46	−10.08
GO:0045165	Cell fate commitment	3.81	−11.72	−9.42
GO:0048513	Animal organ development	5.03	−9.78	−7.78
GO:0045787	Positive regulation of cell cycle	1.78	−9.23	−7.29
GO:0010608	Post-transcriptional regulation of gene expression	3.45	−8.97	−7.05
GO:0050793	Regulation of the developmental process	7.26	−8.80	−6.89

GO	Description	% in GO	Log10 (*p*-value)	Log10 (*q*-value)
GO:0030703	Eggshell formation	0.96	−8.42	−6.43
GO:0018996	Molting cycle, collagen and cuticulin-based cuticle	2.46	−7.78	−5.83
GO:0042127	Regulation of cell population proliferation	1.27	−7.45	−5.63
GO:0051128	Regulation of cellular component organization	6.83	−7.33	−5.41
GO:0045595	Regulation of cell differentiation	2.79	−7.29	−5.48
GO:0032880	Regulation of protein localization	2.59	−7.16	−5.36

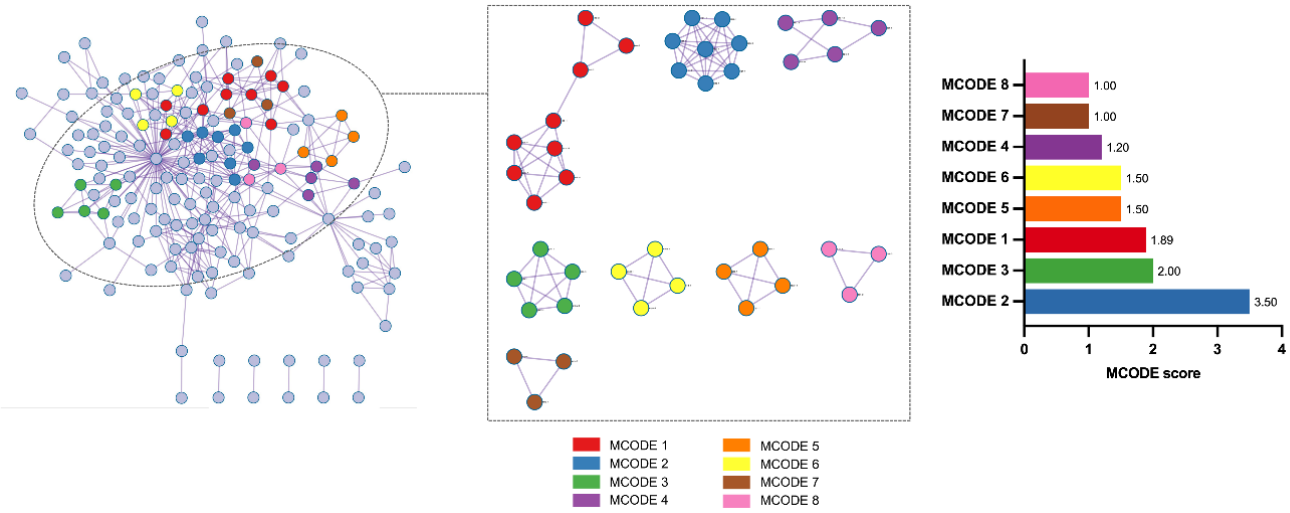

Figure 5 The PPI network was generated through Metascape (https://metascape.org) and visualized in Cytoscape (https://cytoscape.org), with clusters represented by MCODE ID-based color coding.

Table 2 Overlapping protein functional complexes in 6-OHDA- and reserpine-induced groups analyzed by Metascape.

Component	Annotation	Gene symbol	Biological significance linked to neurodegeneration
MCODE 1 & 7	**cel00071:** Fatty acid degradation **cel01212:** Fatty acid metabolism **R-CEL-450513:** Tristetraprolin (TTP, ZFP36) binds and destabilizes mRNA	*ech-9, imb-2, jnk-1, ech-4, oma-2, acs-16, ech-7, mak-2, acdh-1, mrp-4, mrp-2, mrp-7*	Dysregulated fatty acid metabolism disrupts neuronal membrane fluidity, impairs axonal growth, and alters lipid-mediated signaling, thereby contributing to neurotoxicity and the development of neurodegenerative disorders [27].
MCODE 2	**GO:0017148:** Negative regulation of translation **GO:0051248:** Negative regulation of protein metabolic process **GO:0006417:** Regulation of translation	*cgh-1, ifet-1, lin-41, oma-1, car-1, cpb-3, cpb-1, fog-1*	Protein synthesis modulation represents a fundamental cellular stress response, where translational repression functions as an adaptive mechanism to conserve energy and redirect resources toward protective and repair processes [28].
MCODE 3	**GO:0006541:** Glutamine metabolic process **GO:0009064:** Glutamine family amino acid metabolic process	*gln-1, gln-5, gfat-1, glna-3, gfat-2*	Dysregulation of glutamate homeostasis can result in excitotoxicity and neuronal death [29], while glutamate uptake also

Component	Annotation	Gene symbol	Biological significance linked to neurodegeneration
	cel00250: Alanine, aspartate and glutamate metabolism		serves as a crucial precursor for neuronal glutathione biosynthesis [30]
MCODE 4	**GO:0006672:** Ceramide metabolic process **cel00600:** Sphingolipid metabolism **GO:0006665:** Sphingolipid metabolic process	*rpn-1, mlt-3, che-13, abu-14, abu-8*	Alterations in ceramide and sphingolipid metabolism have been implicated in multiple neurodegenerative diseases, as these lipids regulate critical signaling pathways, including Akt/protein kinase B, NF-κB, FOXO, and AP-1 [31].
MCODE 5	**GO:0016441:** Post-transcriptional gene silencing **GO:0035194:** Regulatory ncRNA-mediated post-transcriptional gene silencing **GO:0031047:** Regulatory ncRNA-mediated gene silencing	*asm-3, gba-1, lagr-1, cgt-1*	Post-transcriptional mechanisms such as gene silencing enable rapid cellular adaptation to environmental stressors without initiating new transcription, offering an energy-efficient survival strategy [32].
MCODE 6	**R-CEL-9754706:** Atorvastatin ADME **R-CEL-189483:** Heme degradation **R-CEL-189445:** Metabolism of porphyrins	*wago-1, sid-1, ergo-1, hrde-1*	Deficiencies in porphyrin metabolism lead to the accumulation of toxic porphyrin precursors, which impair cellular respiration and oxygen transport [33].
MCODE 8	**GO:0005879:** Axonemal microtubule **GO:0030036:** Actin cytoskeleton organization **GO:0009792:** Egg hatching	*tba-5, act-2, ssl-1*	Disruption of cytoskeletal organization is a key contributor to neurodegeneration. The neuronal cytoskeleton, composed of protein filaments essential for maintaining cell shape, axonal transport, and synaptic integrity, when perturbed, initiates a cascade of dysfunctions that accelerate neurodegenerative disease progression [34].

Neurotoxic agents mediated neurobehavioral alteration and DAergic neurodegeneration in *C. elegans*

Dopamine plasticity plays a crucial role in behavioral responses of *C. elegans*, such as ethanol avoidance assays [35]. DAergic neurons were visualized using BY250 strain (*dat-1p::gfp*). In our previous study, exposure to 6-OHDA markedly reduced ethanol avoidance index (EAI) ($p < 0.01$) and significantly decreased GFP-labeled CEP neuronal bodies in BY250 worms ($p < 0.001$) [18], supporting its role in inducing both behavioral impairments and DAergic neurodegeneration. To evaluate whether reserpine obtained similar effects, we assessed these endpoints. Reserpine induction led to a significant reduction in EAI (-0.51 ± 0.06, $p < 0.01$) compared with the control (-0.03 ± 0.08) (**Figure 6(A)**). In contrast, analysis of BY250 worms indicated that reserpine did not significantly affect CEPs DAergic neuronal viability ($p = 0.0625$) (**Figure 6(B)**). Collectively, these findings indicate that, unlike 6-OHDA exposure, reserpine disrupts behavioral performance without inducing DAergic neurodegeneration in *C. elegans*.

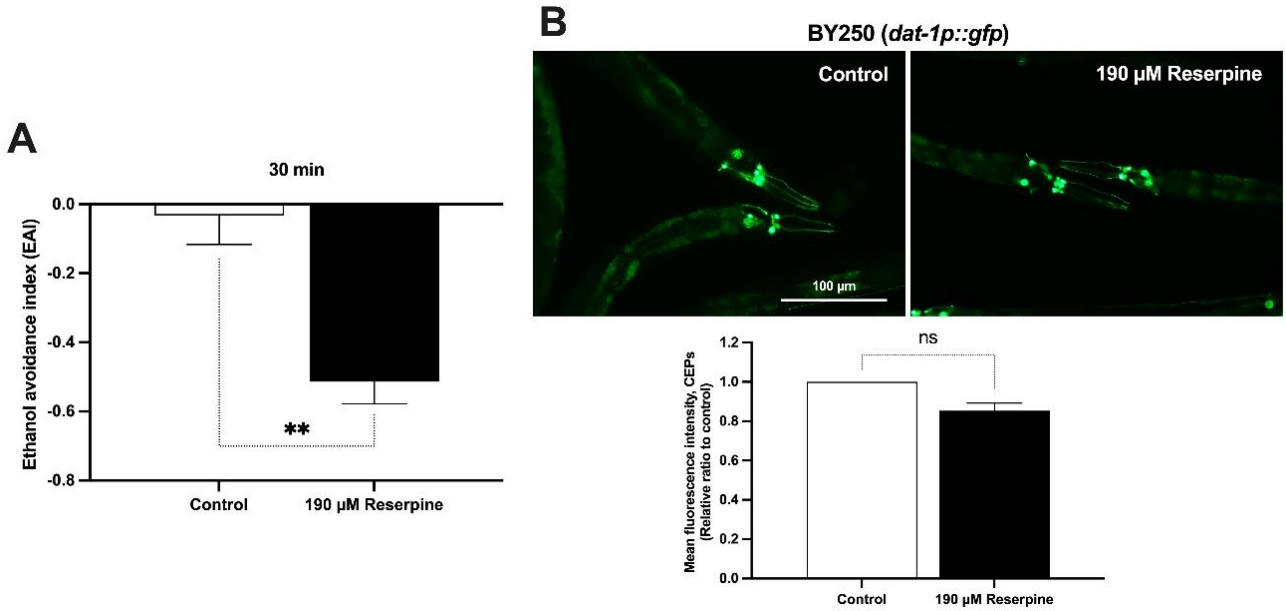

Figure 6 Reserpine-induced toxicity altered neurobehavioral function in ethanol avoidance assay without inducing DAergic neurodegeneration in *C. elegans*. (A) Ethanol avoidance index (EAI) was measured as part of the neurobehavioral assessment (N = 50 - 100 worms per group). (B) CEPs DAergic neurons were visualized using the BY250 strain (*dat-1p::gfp*) (N = 15 worms per group). Results are presented as the mean ± SEM from 3 independent experiments. Statistical significance was determined relative to the control threshold ($^{**}p < 0.01$), with non-significant differences indicated as ns.

Discussion

Whole-genome transcriptome sequencing of *C. elegans* exposed to 6-OHDA and reserpine provides a comprehensive overview of their distinct and overlapping neurotoxic effects. Comparative transcriptomic analysis revealed that although both neurotoxicants exhibit some common fundamental mechanisms, they also exert distinct effects on cellular and stress response pathways related to neurodegeneration.

Previous studies have reported that 6-OHDA is significantly associated with ROS generation, DNA damage, and the activation of PUMA (p53 upregulated modulator of apoptosis), a transcriptional target of p53 [36]. These mechanisms collectively contribute to pathways that either facilitate DNA repair or promote apoptosis [36,37]. Additionally, proteasome-mediated ubiquitination is enriched, highlighting the cellular response to protein misfolding and oxidative damage. Ubiquitin-proteasome system (UPS) is crucial for protein homeostasis by eliminating damaged proteins and preventing aggregate formation [38]. In our study, GO enrichment of the 6-OHDA-induced model reveals a strong downregulation of ribosomal/proteasomal function and protein metabolic processes. Previous study demonstrated that LC-MS/MS proteomic analysis of 6-OHDA-treated differentiated SH-SY5Y neuronal cells shows a significant downregulation of ribosomal/proteasomal proteins. These suggest ribosomal/proteasomal dysfunction associated with unfolded/misfolded protein responses, resulting in an apoptotic induction and neurodegeneration [39]. Moreover, KEGG pathway analysis confirms enrichment in neurodegeneration-associated pathways, including ALS, AD, and PD, with abnormal processes such as impaired protein clearance cascades, oxidative and endoplasmic reticulum (ER) stress, and mitochondrial dysfunction. These results further associate the 6-OHDA-induced *C. elegans* model with human neurodegenerative pathogenesis [40].

Previous studies have demonstrated that induction of 2 mg/L reserpine to zebrafish affects genes enriched in DAergic synapses, voltage-gated ion channels, and Wnt signaling pathways, contributing to depression-like

phenotypes [41]. Similarly, 60 μM reserpine is found to induce DAergic neuronal loss in CEPs of the BY200 *C. elegans* strain, a change that correlated with an increased locomotion rate on food and decreased dopamine levels [10,19]. In the present study, exposure to 190 μM reserpine affects dopamine-dependent behavioral deficits without causing DAergic neuronal loss. Consistent with previous findings, although reserpine recapitulates certain Parkinsonian clinical features and biochemical PD alterations, it does not directly induce DAergic neuronal death [42]. Transcriptomic analysis, in comparison to the 6-OHDA-induced model, revealed that reserpine toxicity predominantly downregulates genes associated with neuropeptide signaling while upregulating genes related to the structural constituents of the cuticle. These findings suggest that reserpine toxicity primarily disrupts neurotransmitter release and neuroendocrine function, thereby affecting neurodevelopment, neuroendocrine communication, and neurotransmitter homeostasis [43, 44]. Additionally, upregulation of structural cuticle genes, including *col*, *nas*, and *dpy*, which are involved in cuticle synthesis and integrity, reflects enhanced collagenous component synthesis and alterations in cuticle organization, particularly under acidic stress and in response to pH change [45]. Moreover, KEGG pathway analysis suggests robust changes in metabolism, such as increased tyrosine metabolism (**Supplementary material 4**) to compensate for depleted catecholamine neurotransmitter storage, like dopamine, caused by a stress condition [46]. Tyrosine is the precursor for synthesizing catecholamine neurotransmitters, including dopamine, norepinephrine, and epinephrine [47]. Additionally, the reserpine-induced model exhibits a metabolic shift toward branched-chain amino acid (BCAA) catabolism, particularly valine, leucine, and isoleucine, as well as pathways linked to fatty acid degradation [48,49]. Upregulation of BCAA and fatty acid catabolic processes is typically observed under conditions of limited cellular energy, suggesting a compensatory mechanism aimed at sustaining energy homeostasis during dopamine depletion-induced cellular stress [48,49]. While VMAT2 blockade by reserpine induces these metabolic adaptations [6], degeneration-associated signatures of reserpine were less evident compared to the 6-OHDA model. From a pharmacological perspective, these findings are consistent with the mechanism of reserpine, which reduces presynaptic monoamines and is the basis for its antihypertensive properties and the risk of depression through modulation of neurosignaling pathways [6, 7]. Moreover, transcriptomic analyses reveal alterations in structural, signaling, and metabolic gene networks in *C. elegans*, which may contribute to the onset of neurobehavioral deficits and progression of neurodegenerative processes. Interestingly, both neurotoxicants significantly affect the Wnt signaling pathways (**Supplementary material 2** and **4**). Dysregulation of Wnt/β-catenin signaling has been implicated in multiple neurodegenerative disorders. In this pathway, cytoplasmic β-catenin accumulates and translocates into the nucleus, where it interacts with Lef/Tcf transcription factors to stimulate over 50 Wnt target genes that are essential for neurogenesis, apoptosis, and inflammation [50]. These findings indicate potential target pathways for exploring diseases related to neurotoxicants and aim at highlighting novel therapeutic targets involved in disease mitigation pathways for further studies.

Metascape and MCODE analyses additionally reveal common pathological mechanisms between 6-OHDA and reserpine, especially involving various biological processes and metabolic regulation. Negative regulation of protein metabolism appears as a key cellular stress response, functioning as an adaptive mechanism to conserve energy by suppressing protein synthesis [28]. Consistent with this, previous studies have shown that phosphorylation of eukaryotic initiation factor 2α (eIF2α) during the integrated stress response (ISR) inhibits overall translation while specifically promoting synthesis of stress-adaptive proteins, such as transcription factor 4 (ATF4), involved in cell recovery and survival [51]. Post-transcriptional regulation, including gene silencing and mRNA degradation, additionally contributes to adaptation under stress by altering gene expression [32]. From a pharmacological perspective, agents that modify the ISR pathway, like small-molecule inhibitors targeting eIF2α phosphatases, are currently investigated for their potential neuroprotective roles, highlighting the translational relevance [52]. Disruption of cell cycle regulation is also implicated in neurodegeneration. Although terminally differentiated neurons normally exist in the quiescent

G0 phase, exposure to neurotoxic substances can trigger an abnormal re-entry into the cell cycle [53]. For instance, 6-OHDA has been reported to induce S-phase arrest through ROS-mediated DNA damage in PC12 cells [54], whereas reserpine leads to a sub-G1 population indicative of apoptosis-related cell cycle interruption in SH-SY5Y cells [6, 55]. This aberrant regulation contributes substantially to neuronal loss in PD and AD. Pharmacologically, this suggests that both ROS overproduction, damage to DNA, and disruption of cell cycle checkpoints are critical factors contributing to neurodegenerative disorders. Additionally, glutamate/glutamine metabolism is involved in neurodegeneration, highlighting its important function in synaptic neurotransmission, excitotoxicity, signaling of ionotropic glutamate N-methyl-D-aspartate (NMDA) receptors, and energy homeostasis. Impairment of this pathway leads to synaptic dysfunction and neuronal injury in neurodegenerative disorders [29]. This process is related to and supported by clinical evidence on the pharmacological modulation of glutamatergic signaling, such as NMDA receptor antagonists (e.g., memantine in AD) [56]. Disruptions in lipid metabolism also appear to be a convergent mechanism of neurotoxicity. Lipidomic studies have reported changes in various lipid families, including free fatty acids (FFAs), cholesterol esters (CEs), triglycerides (TGs), and eicosanoids, during 6-OHDA-induced DAergic neurodegeneration [57]. Likewise, reserpine exposure in zebrafish alters brain metabolites such as glutamate, glutamine, lactate, and glutathione, leading to oxidative stress, metabolic imbalance, and indirect interference with fatty acid metabolism [58]. These provide the pharmacological significance of drugs that act on lipid peroxidation. Common pathological mechanisms observed following 6-OHDA and reserpine exposure indicate fundamental adaptations in dopamine metabolism and associated neurobehavioral alterations in PD pathology, thereby highlighting preserved targets in pathways and mechanisms linked to PD pathogenesis.

This study employs transcriptomic sequencing to investigate neurotoxicant-induced PD pathologies in *C. elegans* model. This approach offers a valuable high-throughput system for identifying compounds that can alter neurotoxicity mediated by molecular pathways [13,17]. Nevertheless, certain limitations exist, as *C. elegans* lacks several mammalian-specific anatomical structures, including a circulatory system, blood-brain barrier (BBB), hepatic metabolism, and renal filtration [59]. Therefore, findings obtained from this model should be further validated in complementary systems, including mammalian or rodent models [60], to confirm their conservation across species, involvement of organ-specific processes related to neurodegeneration, and translational relevance to human neurodegenerative disorders. Importantly, transcriptomic profiling provides a deeper understanding of the mechanisms by which 6-OHDA and reserpine exert their effects in establishing PD models, thereby clarifying their role in recapitulating disease-relevant neurodegenerative processes. Collectively, this study provides important insights into the molecular mechanisms of neurodegeneration induced by these compounds, thereby enhancing our understanding of disease pathogenesis and related pathways. Moreover, these findings not only highlight potential pharmacological targets, including transcription repression function, post-transcriptional mechanisms, glutamatergic modulators, and fatty acid regulators, but also provide their value in guiding the discovery and development of therapeutic candidates in future research.

Conclusions

This comparative transcriptomic analysis of 6-OHDA and reserpine in *C. elegans* establishes a molecular basis for understanding their neurotoxic effects. This study reveals that each compound induces a unique primary transcriptomic profile: 6-OHDA predominantly impacts ribosomal/proteasomal function and pathways linked to neurodegeneration, whereas reserpine primarily influences the extracellular region, the neuropeptide signaling, and metabolic pathways. Despite these differences, both neurotoxicants converge on overlapping mechanisms, including cell development, reproductive systems, cytoskeletal arrangement, cell cycle regulation, multiple metabolic pathways, and post-transcriptional regulation, as identified by Metascape and MCODE components. Furthermore, reserpine exposure causes dopamine-dependent behavioral deficit without affecting DAergic neuronal damage. Collectively, these findings suggest that the identified pathways represent valuable insights into the molecular mechanisms of neurotoxicity and identify potential pharmacological targets and pathways

for future neurotoxicity research involved in PD pathogenesis.

Acknowledgements

This work was supported by Pathumthani University (No. RIC67002: year 2024) and Mahidol University (MU's Strategic Research Fund: fiscal year 2023). *C. elegans* strains utilized were obtained from the *Caenorhabditis* Genetics Center (CGC), supported by the NIH Office of Research Infrastructure Programs (P40 OD010440). We sincerely acknowledge the Cell and Tissue Biology Research Unit (B101), KM's *C. elegans* Laboratory Unit, and the core facility of the Department of Anatomy, Faculty of Science, Mahidol University, Thailand, for supplying essential laboratory resources. BY250 strain was kindly provided by Prof. Randy Blakely, Florida Atlantic University, USA, for which we express our gratitude.

Declaration of Generative AI in Scientific Writing

During the preparation of this work, the authors used ChatGPT and Grammarly to enhance clarity and linguistic quality. After using these tools, the authors reviewed and edited the content as necessary and took full responsibility for the final publication.

CRediT Author Statement

Sukrit Promtang: Writing - original draft, Conceptualization, Funding acquisition, Resources, Investigation, Data curation, Formal analysis. **Tanatcha Sanguanphun:** Writing - review & editing, Visualization, Resources, Methodology, Investigation. **Darunee Rodma:** Writing - review & editing, Funding acquisition, Visualization, Validation. **Rungsarit Sunan:** Writing - review & editing, Funding acquisition, Visualization, Validation. **Apinya Sayinta:** Writing - review & editing, Funding acquisition, Visualization, Validation. **Thanes Fuangfoo:** Writing - review & editing, Visualization, Validation. **Nattapong Snitmatjaro:** Writing - review & editing, Visualization, Validation. **Chaiyo Chaichantipyuth:** Writing - review & editing, Visualization, Validation. **Narisa Kamkaen:** Writing - review & editing, Visualization, Validation. **Krai Meemon:** Writing - review & editing, Supervision, Validation, Resources, Funding acquisition, Project administration. **Pawanrat Chalorak:** Writing - review & editing, Supervision, Validation, Resources, Investigation, Project administration

References

[1] DM Wilson, MR Cookson, L Van Den Bosch, H Zetterberg, DM Holtzman and I Dewachter. Hallmarks of neurodegenerative diseases. *Cell* 2023; **186(4)**, 693-714.

[2] E Guatteo, N Berretta, V Monda, A Ledonne and NB Mercuri. Pathophysiological features of nigral dopaminergic neurons in animal models of Parkinson's disease. *International Journal of Molecular Sciences* 2022; **23(9)**, 4508.

[3] National Research Council (US) Committee on Neurotoxicology and Models for Assessing Risk. *Environmental neurotoxicology.* National Academies Press, Washington DC, 1992.

[4] AY Altahrawi, AW James and ZA Shah. The role of oxidative stress and inflammation in the pathogenesis and treatment of vascular dementia. *Cells* 2025; **14(8)**, 609.

[5] A Schober. Classic toxin-induced animal models of Parkinson's disease: 6-OHDA and MPTP. *Cell and Tissue Research* 2004; **318(1)**, 215-224.

[6] Y Li, Q Yin, B Wang, T Shen, W Luo and T Liu. Preclinical reserpine models recapitulating motor and non-motor features of Parkinson's disease: Roles of epigenetic upregulation of alpha-synuclein and autophagy impairment. *Frontiers in Pharmacology* 2022; **13**, 944376.

[7] M Govindarajulu, T Shankar, S Patel, M Fabbrini, A Manohar, S Ramesh and P Boralingaiah. *Reserpine-induced depression and other neurotoxicity: A monoaminergic hypothesis. In*: Medicinal herbs and fungi: Neurotoxicity vs. Neuroprotection. Springer, Cham, Switzerland, 2021, p. 293-313.

[8] AC Lima, VS Bioni, MS Becegato, Y Meier, DMG Cunha, NA Aguiar, N Gonçalves, FF Peres, AW Zuardi, JEC Hallak, JEC Hallak, A Crippa, JA Crippa, SS Smaili, SS Smaili, VC Abilio,VC Abilio, RH Silva and RH Silva. Preventive beneficial effects of cannabidiol in a reserpine-induced progressive model of parkinsonism. *Frontiers in Pharmacology* 2025; **16**, 1539783.

[9] J Lama, Y Buhidma, EJR Fletcher and S Duty. Animal models of Parkinson's disease: A guide to

selecting the optimal model for your research. *Neuronal Signaling* 2021; **5(4)**, NS20210026.

[10] P Reckziegel, P Chen, S Caito, P Gubert, FAA Soares, R Fachinetto and M Aschner. Extracellular dopamine and alterations on dopamine transporter are related to reserpine toxicity in *Caenorhabditis elegans*. *Archives of Toxicology* 2016; **90(3)**, 633-645.

[11] A Dovonou, C Bolduc, V Soto Linan, C Gora, MR Peralta and M Lévesque. Animal models of Parkinson's disease: Bridging the gap between disease hallmarks and research questions. *Translational Neurodegeneration* 2023; **12(1)**, 36.

[12] S Das, KS Saili and RL Tanguay. *Nonmammalian models in toxicology screening*. *In*: Encyclopedia of toxicology. 3rd ed. Elsevier, Amsterdam, Netherlands, 2014, p. 609-613.

[13] J Li and W Le. Modeling neurodegenerative diseases in *Caenorhabditis elegans. Experimental Neurology* 2013; **250**, 94-103.

[14] X Chen, JW Barclay, RD Burgoyne and A Morgan. Using *C. elegans* to discover therapeutic compounds for ageing-associated neurodegenerative diseases. *Chemistry Central Journal* 2015; **9(1)**, 65.

[15] M Maulik, S Mitra, A Bult-Ito, BE Taylor and EM Vayndorf. Behavioral phenotyping and pathological indicators of Parkinson's disease in C. elegans models. *Frontiers in Genetics* 2017; **8**, 77.

[16] CH Lai, CY Chou, LY Ch'ang, CS Liu and W Lin. Identification of novel human genes evolutionarily conserved in Caenorhabditis elegans by comparative proteomics. *Genome Research* 2000; **10(5)**, 703-713.

[17] X Chen, JW Barclay, RD Burgoyne and A Morgan. Using *C. elegans* to discover therapeutic compounds for ageing-associated neurodegenerative diseases. *Chemistry Central Journal* 2015; **9**, 65.

[18] S Promtang, T Sanguanphun, P Chalorak, D Rodma, R Sunan, LS Pe and N Niamnont. Neurorestorative properties of 2-butoxytetrahydrofuran from *Holothuria scabra* via activation of stress resistance and detoxification in a 6-OHDA-induced *C. elegans* model of Parkinson's disease. *Biomedicine & Pharmacotherapy* 2025; **188**, 118158.

[19] E da Cruz Guedes, AG Erustes, AHFF Leão, CA Carneiro, VC Abílio, AW Zuardi, JEC Hallak, JA Crippa, C Bincoletto, SS Smaili, P Reckziegel and GJS Pereira. Cannabidiol recovers dopaminergic neuronal damage induced by reserpine or α-synuclein in *Caenorhabditis elegans. Neurochemical Research* 2023; **48(8)**, 2390-2405.

[20] S Promtang, T Sanguanphun, P Chalorak, LS Pe, N Niamnont, P Sobhon and K Meemon. 2-butoxytetrahydrofuran, isolated from *Holothuria scabra*, attenuates aggregative and oxidative properties of α-synuclein and alleviates its toxicity in a transgenic *Caenorhabditis elegans* model of Parkinson's disease. *ACS Chemical Neuroscience* 2024; **15(11)**, 2182.

[21] Y Zhou, B Zhou, L Pache, M Chang, AH Khodabakhshi, O Tanaseichuk, C Benner and SK Chanda. Metascape provides a biologist-oriented resource for the analysis of systems-level datasets. *Nature Communications* 2019; **10(1)**, 1523.

[22] J Kohen. A coefficient of agreement for nominal scale. *Educational and Psychological Measurement* 1960; **20**, 37-46.

[23] A Chatr-Aryamontri, R Oughtred, L Boucher, J Rust, C Chang, NK Kolas, L O'Donnell, S Oster, C Theesfeld, A Sellam, C Stark, BJ Breitkreutz, K Dolinski and M Tyers. The BioGRID interaction database: 2017 update. *Nucleic Acids Research* 2017; **45(D1)**, D369-D379.

[24] GD Bader and CW Hogue. An automated method for finding molecular complexes in large protein interaction networks. *BMC Bioinformatics* 2003; **4(1)**, 2.

[25] P Shannon, A Markiel, O Ozier, NS Baliga, JT Wang, D Ramage, N Amin, B Schwikowski and T Ideker. Cytoscape: A software environment for integrated models of biomolecular interaction networks. *Genome Research* 2003; **13(11)**, 2498-2504.

[26] JF Cooper, DJ Dues, KK Spielbauer, E Machiela, MM Senchuk and JM Van Raamsdonk. Delaying aging is neuroprotective in Parkinson's disease: A genetic analysis in *C. elegans* models. *NPJ Parkinson's Disease* 2015; **1(1)**, 15022.

[27] I Alecu and SAL Bennett. Dysregulated lipid metabolism and its role in α-synucleinopathy in Parkinson's disease. *Frontiers in Neuroscience* 2019; **13**, 328.

[28] S Yamasaki and P Anderson. Reprogramming mRNA translation during stress. *Current Opinion in Cell Biology* 2008; **20(2)**, 222-226.

[29] JV Andersen, KH Markussen, E Jakobsen, A Schousboe, HS Waagepetersen, PA Rosenberg and BI Aldana. Glutamate metabolism and recycling at the excitatory synapse in health and neurodegeneration. *Neuropharmacology* 2021; **196**, 108719.

[30] A Vaglio-Garro, AV Kozlov, YD Smirnova and A Weidinger. Pathological interplay between inflammation and mitochondria aggravates glutamate toxicity. *International Journal of Molecular Sciences* 2024; **25(4)**, 2276.

[31] K Czubowicz, H Jęśko, P Wencel, WJ Lukiw and RP Strosznajder. The role of ceramide and sphingosine-1-phosphate in Alzheimer's disease and other neurodegenerative disorders. *Molecular Neurobiology* 2019; **56(8)**, 5436-5455.

[32] M Hernández-Elvira and P Sunnerhagen. Post-transcriptional regulation during stress. *FEMS Yeast Research* 2022; **22(1)**, foac025.

[33] D Maitra, JB Cunha, JS Elenbaas, HL Bonkovsky, JA Shavit and MB Omary. Porphyrin-induced protein oxidation and aggregation as a mechanism of porphyria-associated cell injury. *Cellular and Molecular Gastroenterology and Hepatology* 2019; **8(4)**, 535-548.

[34] JC Vickers, AE King, A Woodhouse, MT Kirkcaldie, JA Staal, GH McCormack, CA Blizzard, REJ Musgrove, S Mitew, Y Liu, JA Chuckowree, O Bibari a TC Dickson Axonopathy and cytoskeletal disruption in degenerative diseases of the central nervous system. *Brain Research Bulletin* 2009; **80(4-5)**, 217-223.

[35] JF Cooper and JM Van Raamsdonk. Modeling Parkinson's disease in *C. elegans. Journal Of Parkinson's Disease* 2018; **8(1)**, 17-32.

[36] AI Bernstein, SP Garrison, GP Zambetti and KL O'Malley. 6-OHDA generated ROS induces DNA damage and p53-and PUMA-dependent cell death. *Molecular Neurodegeneration* 2011; **6(1)**, 2.

[37] M Li. The role of P53 up-regulated modulator of apoptosis (PUMA) in ovarian development, cardiovascular and neurodegenerative diseases. *Apoptosis* 2021; **26(5)**, 235-247.

[38] R Kandel, J Jung and S Neal. Proteotoxic stress and the ubiquitin proteasome system. *Seminars in Cell & Developmental Biology* 2024; **156**, 107-120.

[39] KB Magalingam, SD Somanath, P Ramdas, N Haleagrahara and AK Radhakrishnan. 6-hydroxydopamine induces neurodegeneration in terminally differentiated SH-SY5Y neuroblastoma cells via enrichment of the nucleosomal degradation pathway: A global proteomics approach. *Journal of Molecular Neuroscience* 2022; **72(5)**, 1026-1046.

[40] N Pathak, SK Vimal, I Tandon, L Agrawal, C Hongyi and S Bhattacharyya. Neurodegenerative disorders of alzheimer, parkinsonism, amyotrophic lateral sclerosis and multiple sclerosis: An early diagnostic approach for precision treatment. *Metabolic Brain Disease* 2022; **37(1)**, 67-104.

[41] Y Luo, M Zheng, Z Su, C Cai and X Li. Transcriptome profile of reserpine-induced locomotor behavioral changes in zebrafish (*Danio rerio*). *Progress in Neuro-Psychopharmacology and Biological Psychiatry* 2024; **129**, 110874.

[42] S Duty and P Jenner. Animal models of Parkinson's disease: A source of novel treatments and clues to the cause of the disease. *British Journal of Pharmacology* 2011; **164(4)**, 1357-1391.

[43] F Sun, L Xia, B Wang, Y Liu, X Cui, H Kang, R Stoika, K Liu and M Jin. Reserpine causes neuroendocrine toxicity, inducing impairments in cognition via disturbing hypothalamic-pituitary-thyroid axis in zebrafish. *NeuroSci* 2025; **6(2)**, 28.

[44] AHFF Leão, AJ Sarmento-Silva, JR Santos, AM Ribeiro and RH Silva. Molecular, neurochemical, and behavioral hallmarks of reserpine as a model for Parkinson's disease: New perspectives to a long-standing model. *Brain Pathology* 2015; **25(4)**, 377-390.

[45] Y Cong, H Yang, P Zhang, Y Xie, X Cao and L Zhang. Transcriptome analysis of the nematode Caenorhabditis elegans in acidic stress

environments. *Frontiers in Physiology* 2020; **11**, 1107.

[46] LK Ong, L Sominsky, PW Dickson, DM Hodgson and PR Dunkley. The sustained phase of tyrosine hydroxylase activation *in vivo*. *Neurochemical Research* 2012; **37(9)**, 1938-1943.

[47] SC Daubner, T Le and S Wang. Tyrosine hydroxylase and regulation of dopamine synthesis. *Archives of Biochemistry and Biophysics* 2011; **508(1)**, 1-12.

[48] S Zou, T Lang, B Zhang, K Huang, L Gong, H Luo, W Xu and X He. Fatty acid oxidation alleviates the energy deficiency caused by the loss of MPC1 in MPC1+/− mice. *Biochemical and Biophysical Research Communications* 2018; **495(1)**, 1008-1013.

[49] BH Choi, S Hyun and SH Koo. The role of BCAA metabolism in metabolic health and disease. *Experimental & Molecular Medicine* 2024; **56(7)**, 1552-1559.

[50] AA Anand, M Khan, MV and D Kar. The molecular basis of Wnt/β-catenin signaling pathways in neurodegenerative diseases. *International Journal of Cell Biology* 2023; **2023(1)**, 9296092.

[51] PD Lu, HP Harding and D Ron. Translation reinitiation at alternative open reading frames regulates gene expression in an integrated stress response. *The Journal of Cell Biology* 2004; **167(1)**, 27-33.

[52] MA Bravo-Jimenez, S Sharma and S Karimi-Abdolrezaee. The integrated stress response in neurodegenerative diseases. *Molecular Neurodegeneration* 2025; **20(1)**, 20.

[53] JM Frade and MC Ovejero-Benito. Neuronal cell cycle: The neuron itself and its circumstances. *Cell Cycle* 2015; **14(5)**, 712-720.

[54] LW Hu, JH Yen, YT Shen, KY Wu and MJ Wu. Luteolin modulates 6-hydroxydopamine-induced transcriptional changes of stress response pathways in PC12 cells. *PloS One* 2014; **9(5)**, e97880.

[55] R Park, KII Lee, H Kim, M Jang, TKQ Ha, WK Oh and J Park. Reserpine treatment activates AMP activated protein kinase (AMPK). *Natural Product Sciences* 2017; **23(3)**, 157-161.

[56] C Volbracht, J Van Beek, C Zhu, K Blomgren and M Leist. Neuroprotective properties of memantine in different *in vitro* and *in vivo* models of excitotoxicity. *European Journal of Neuroscience* 2006; **23(10)**, 2611-2622.

[57] J Qiu, G Peng, Y Tang, S Li, Z Liu, J Zheng, Y Wang, H Liu, H Liu, L Wei, Y Su, Y Lin, W Dai, Z Zhang, X Chen, L Ding, W Guo, X Zhu, P Xu and M Mo. Lipid profiles in the cerebrospinal fluid of rats with 6-hydroxydopamine-induced lesions as a model of Parkinson's disease. *Frontiers in Aging Neuroscience* 2023; **14**, 1077738.

[58] F Zakaria, MT Akhtar, WN Wan Ibrahim, N Abu Bakar, A Muhamad, S Shohaimi, M Maulidiani, H Ahmad, IS Ismail and K Shaari. Perturbations in amino acid metabolism in reserpine-treated zebrafish brain detected by 1H nuclear magnetic resonance-based metabolomics. *Zebrafish* 2021; **18(1)**, 42-54.

[59] C Weinhouse, L Truong, JN Meyer and P Allard. *Caenorhabditis elegans* as an emerging model system in environmental epigenetics. *Environmental and Molecular Mutagenesis* 2018; **59(7)**, 560-575.

[60] G Khanjari, I Mohammadzadeh, Y Khakpour, M Nikoohemmat, M Norouzian, S Parvardeh, A Beirami, M Hasanzadeh, NB Amini, Z Niakan, GH Meftahi, A Seraj, AH Tajik, H Hemmatparast, R Bahar, MH Hajali, H Karbalaei-Musa, AH Bayat, MH Moghaddam, M Sani and A Aliaghae. Neuroprotective effects of the elderberry diet on the methamphetamine-induced toxicity in rats: A behavioral, electrophysiological, and histopathological study. *3 Biotech* 2025; **15(5)**, 122.